Supplemental Material for "A continuum limit for dense spatial networks"

Sidney Holden[1,2*] and Geoffrey Vasil[2†]
[1] *Center for Computational Biology, Flatiron Institute, New York, NY, USA 10010 and*
[2] *School of Mathematics and Maxwell Institute for Mathematical Sciences, The University of Edinburgh, EH9 3FD, United Kingdom*

Appendix A: Nonlinear eigenvalue problem (NEP)

For $\lambda = k^2$, the system has the general form,

$$L(k)\cdot f(V) \;=\; 0 \qquad \text{where} \qquad L_{vw}(k) \;=\; \begin{cases} \sum_{w\sim v} K_{vw}C_{vw}\cot(kK_{vw}/C_{vw}\ell_{vw}) & \text{if } \; w=v, \\ -K_{vw}C_{vw}\csc(kK_{vw}/C_{vw}\ell_{vw}) & \text{if } \; w\sim v, \\ 0 & \text{otherwise.} \end{cases} \tag{A1}$$

The eigenvector, $f(V)$, encodes the exact values of the mathematical function $f(x)$ evaluated at the finite set of vertices, V. The $|V|\times|V|$ matrix, $L(k)$, depends nonlinearly on the spectral parameter, k, obstructing standard matrix factorizations like LU or QR. We solve $\det(L(k))=0$, for k with Newton's method using Jacobi's formula for the logarithmic derivative,

$$k_{n+1} \;=\; k_n - \frac{1}{\operatorname{tr}(L(k_n)^{-1}L'(k_n))}, \tag{A2}$$

We compute the derivative, $L'(k)$ analytically from eq. (A1). The main numerical challenge involves calculating the inverse, $L(k)^{-1}$, where we deploy sparse methods. For a given solution, we have $L(k)\cdot f(V)=0$ for nontrivial $f(V)$. Therefore, the minimum singular value vanishes, $\sigma_{\min}=0$. We apply Newton's method directly to

$$\sigma_{\min}(k) \;=\; u^*_{\min}(k)\cdot L(k)\cdot v_{\min}(k) \;=\; 0, \tag{A3}$$

for respective left and right singular vectors $u_{\min}$ and $v_{\min}$. For the derivative, [1] shows that $\sigma'_{\min}(k) = u^*_{\min}(k)\cdot L'(k)\cdot v_{\min}(k)$. Therefore,

$$k_{n+1} \;=\; k_n - \frac{\sigma_{\min}(k_n)}{u^*_{\min}(k_n)\cdot L'(k_n)\cdot v_{\min}(k_n)}. \tag{A4}$$

Recent work [1, 2] shows approximating $u_{\min}$ and $v_{\min}$ by inverse iteration at each step preserves local quadratic convergence for simple eigenvalues. For symmetric $L(k)$, $u_{\min}=v_{\min}\in\mathbb{R}^{|V|}$, therefore:

1. Initiate with k and calculate u,σ,σ'.
2. Until convergence:
   (a) $k \leftarrow k-\sigma/\sigma'$
   (b) $u \leftarrow L(k)^{-1}u$
   (c) $u \leftarrow u/\|u\|$
   (d) $\sigma \leftarrow u\cdot L(k)\cdot u$
   (e) $\sigma' \leftarrow u\cdot L'(k)\cdot u$.

For step (b), we use a single sparse linear solve, not the full inverse, $L(k)^{-1}$. Step (c) is not required mathematically but prevents eventual numerical overflow/underflow. The algorithm trivially parallelizes over different k solutions.

* sholden@flatironinstitute.org
† gvasil@ed.ac.uk

Appendix B: Multi-edges

Consider a graph with $|G| = g$ and the following $g \times g$ block-structured adjacency matrix,

$$\mathcal{A} = \begin{bmatrix} A & B \\ B^\top & a \end{bmatrix} \qquad \text{where} \qquad a = \begin{bmatrix} 0 & 1 \\ 1 & 0 \end{bmatrix}, \tag{B1}$$

which singles out two connected vertices, $v \sim w$, with local adjacency matrix, a. The A block is a $(g-2) \times (g-2)$ adjacency matrix for the bulk of the graph, and B is an $(g-2) \times 2$ matrix specifying how v, w connect to the bulk.

Now consider an augmented multi-graph with $g_n = g + 2(n-1)$ vertices and $g_n \times g_n$ adjacency matrix,

$$\mathcal{A}_n = \begin{bmatrix} A & B \otimes 1_n \\ B^\top \otimes 1_n^\top & a \otimes \left(1_n^\top 1_n\right) \end{bmatrix} \qquad \text{where} \qquad 1_n = \begin{bmatrix} 1 & \dots & 1 \end{bmatrix}. \tag{B2}$$

The augmented graph has n identical copies of each v, w with identical connectivity structure to the rest of the graph—the equivalent of making a two-lane segment of the road into a $2n$-lane version of the same segment.

Theorem 1. *Define the $g \times g$ weighted adjacency matrix,*

$$\widetilde{\mathcal{A}}_n = \begin{bmatrix} A & \sqrt{n}\, B \\ \sqrt{n}\, B^\top & n\, a \end{bmatrix}. \tag{B3}$$

For the characteristic polynomials,

$$\det(\mathcal{A}_n - z\, \mathcal{I}_{g_n}) = z^{2(n-1)}\, \det(\widetilde{\mathcal{A}}_n - z\, \mathcal{I}_g). \tag{B4}$$

Proof. Define the following identity matrices: e (2×2); I $((g-2) \times (g-2))$; and I_n $(n \times n)$. Then,

$$\mathcal{A}_n - z\, \mathcal{I}_{g_n} = \begin{bmatrix} A - z\, I & B \otimes 1_n \\ B^\top \otimes 1_n^\top & a \otimes \left(1_n^\top 1_n\right) - z\, e \otimes \mathrm{I}_n \end{bmatrix}. \tag{B5}$$

By the block Schur complement, the full characteristic polynomial,

$$\det(\mathcal{A}_n - z\, \mathcal{I}_{g_n}) \;=\; \det(D_{n,z})\, \det(A - zI - (B \otimes 1_n)\, D_{n,z}^{-1}\, (B^\top \otimes 1_n^\top)), \tag{B6}$$

where

$$D_{n,z} = a \otimes \left(1_n^\top 1_n\right) - z\, e \otimes \mathrm{I}_n, \qquad D_{n,z}^{-1} = -\frac{1}{z^2 - n^2}(n\, z^{-1} e + a) \otimes \left(1_n^\top 1_n\right) - z^{-1} e \otimes \mathrm{I}_n, \tag{B7}$$

which only requires $a^2 = e$ and $1_n 1_n^\top = n$. The matrix $a \otimes \left(1_n^\top 1_n\right)$ has eigenvalues $z = 0, \pm n$ where $D_{n,z}^{-1}$ has poles; $z = 0$ has $2(n-1)$ multiplicity because 1_n is orthogonal to any zero-sum vector. Therefore,

$$\det(D_{n,z}) = z^{2(n-1)}\, (z^2 - n^2). \tag{B8}$$

By direct computation,

$$(B \otimes 1_n)\, D_{n,z}^{-1}\, (B^\top \otimes 1_n^\top) = -\frac{1}{z^2 - n^2}(\, n\, z\, BB^\top + n^2 B\, a\, B^\top), \tag{B9}$$

therefore,

$$\det(\mathcal{A}_n - z\, \mathcal{I}_{g_n}) \;=\; z^{2(n-1)}\, \det(n\, a - z\, e) \left| A - zI + \frac{1}{z^2 - n^2}(\, n\, z\, BB^\top + n^2 B\, a\, B^\top) \right| \tag{B10}$$

$$\;=\; z^{2(n-1)} \begin{vmatrix} A - z\, I & \sqrt{n}\, B \\ \sqrt{n}\, B^\top & n\, a - z\, e \end{vmatrix}. \tag{B11}$$

The last equality follows from Schur complementing off the block where $\det(n\, a - z\, e) = z^2 - n^2$. □

We can summarize the results in a way that is similar to the situation with the Sydney Harbour Bridge. Roads from all over the city meet at a junction that takes you over the bridge in one of $n = 4$ lanes (each way). Once on the bridge, you're required to stay in your chosen lane. After the bridge, you are free to pick any of a large number of roads that take you to the rest of the city. The transport through the bridge is four times larger than it would be with only one lane over the bridge. But the transport through the junctions to the rest of the city is only $2 = \sqrt{4}$ times larger.

Appendix C: Metric tensor comparison

Consider the following ratio for two nearby points, $x \approx y$ on a manifold with distance,

$$S(x,y) \;=\; \frac{(f(x)-f(y))^2}{\mathrm{dist}(x,y)^2}. \tag{C1}$$

For a parameterized curve, $\gamma(t)$, with $x=\gamma(0)$ to $y=\gamma(t)$, as $t\to 0$,

$$S(x,y) \;\approx\; \frac{(v\cdot \mathrm{d}f(x))^2}{v\cdot g(x)\cdot v}, \quad \text{as} \quad y\to x, \tag{C2}$$

with the tangent vector (from x to y), $v(x)=\gamma'(0)$, the local metric tensor, $g(x)$, and the local gradient 1-form,

$$\mathrm{d}f = \sum_{i=1}^{d} \partial_i f \,\mathrm{d}x^i. \tag{C3}$$

The tangent vector, v, is the closest analogue to an edge in a metric graph. By definition,

$$\hat{v}(x) = \frac{v(x)}{\sqrt{v(x)\cdot g(x)\cdot v(x)}}. \tag{C4}$$

Therefore,

$$S(x,y) \;\approx\; (\hat{v}(x)\cdot \mathrm{d}f(x))^2, \quad \text{as} \quad y\to x, \tag{C5}$$

where $\hat{v}(x)$ is "pointing" at y. Now sum $S(x,y)$ over $\deg(x)$ approximately uniformly spaced direction vectors, $\hat{v}(x)$,

$$\sum_{y\sim x} S(x,y) \;\approx\; \sum_{e=1}^{\deg(x)} (\hat{v}_e\cdot \mathrm{d}f(x))^2. \tag{C6}$$

We can approximate the sum with an integral over S^{d-1}. In a local orthogonal basis,

$$g \;=\; \sum_{i=1}^{d} h_i \,\mathrm{d}x^i \otimes \mathrm{d}x^i, \tag{C7}$$

with scale factors $h_i>0,\ \mathrm{d}x^i\cdot\partial_j=\delta^i_j$, and

$$\hat{v}_e = \sum_{i=1}^{d} \frac{\hat{n}_e^i}{\sqrt{h_i}}\,\partial_i, \qquad \text{where} \qquad \sum_{i=1}^{d} (\hat{n}_e^i)^2 \;=\; 1, \tag{C8}$$

Using spherical polar coordinates,

$$\frac{1}{|S^{d-1}|}\int_{S^{d-1}} \hat{n}\otimes\hat{n}\,\mathrm{d}\hat{n} = \frac{1}{d}\,I_d. \tag{C9}$$

Therefore,

$$\frac{1}{|S^{d-1}|}\int_{S^{d-1}} (\hat{v}_{\hat{n}}\cdot \mathrm{d}f(x))^2\,\mathrm{d}\hat{n} \;=\; \frac{1}{d}\sum_i \frac{(\partial_i f)^2}{h_i} \;=\frac{1}{d}\,\mathrm{d}f(x)\cdot g(x)^{-1}\cdot \mathrm{d}f(x). \tag{C10}$$

Therefore,

$$\sum_{y\sim x} S(x,y) \;\approx\; \deg(x)\left\langle (\hat{v}\cdot \mathrm{d}f)^2\right\rangle \;\approx\; \frac{\deg(x)}{d}\,\mathrm{d}f(x)\cdot g(x)^{-1}\cdot \mathrm{d}f(x). \tag{C11}$$

To summarize,

$$\sum_{y\sim x} \frac{(f(x)-f(y))^2}{\ell_{xy}^2} \;\approx\; \frac{\deg(x)}{d}\;\mathrm{d}f(x)\cdot g(x)^{-1}\cdot \mathrm{d}f(x). \tag{C12}$$

If we repeat the calculation instead starting with $(f(x)-f(y))^2/\ell_{xy}$ then we don't know how the lengths depend on $\hat{v}$, and hence the $\hat{n}\in S^2$ parameters. Therefore, we cannot use eq. (C9). However, for constant edge lengths,

$$R(x) \approx \frac{\ell\,\deg(x)}{d}\,g(x)^{-1}, \qquad \mathrm{tr}_g(R(x)) \;=\; \ell\,\deg(x). \tag{C13}$$

Appendix D: Spiderweb

Discrete solution

For the spiderweb, the original graph problem eq. (6) of the Main Text [3] simplifies into decoupled radial systems. In this case, $dr = dr(r)$ takes discrete values on the edges. At a vertex $v(r, \theta)$, edges pointing to neighbors toward and away from the central vertex have lengths $dr_-(r)$ and a $dr_+(r)$ respectively. The Kirchhoff condition is

$$\frac{f_m(r + dr_+) + f_m(r - dr_-)}{2\sin(k\,dr)} + \left[\frac{\cos(m\,d\theta)}{\sin(kr\,d\sigma)} - \cot(kr\,d\sigma) - \frac{\cot(k\,dr_+) + \cot(k\,dr_-)}{2}\right] f_m(r) \;=\; 0, \tag{D1}$$

where $d\sigma = 2\sin(d\theta/2)$ and $|m| \le M = 2\pi/d\theta$. As $dr, d\theta \to 0$ with $\rho = dr/d\theta \sim \mathcal{O}(1)$, eq. (D1) reduces exactly to eq. (22) of the Main Text [3] at leading order. The vertex (with M neighbors) at the origin requires special care. For the discrete case,

$$f_m(0)\cos(k\,dr) - f_m(dr)\,\delta_{m,0} \;=\; 0, \tag{D2}$$

with Kronecker-$\delta_{m,0}$. As $dr \to 0$, the center conditions are

$$f_m(0) \;=\; 0 \quad \text{if} \quad m \neq 0, \tag{D3}$$

$$f_0'(0) \;=\; 0 \quad \text{if} \quad m = 0. \tag{D4}$$

Analyzing the PDE within an ε-ball around the origin produces identical center conditions.

Construction for $\rho(r) = r/\gamma$

y We set $\gamma = 1$ for the example in the Main Text [3]. The relationship $dr = rd\theta$ requires a recurrence relation for constructing the radial distribution of vertices with coordinates $r \in \{r_{V_r-1} = 0,\ \ldots\ ,\ r_0 = 1\}$. Starting from the boundary vertex,

$$r_n \;=\; r_0(1 - d\theta)^n. \tag{D5}$$

For some fixed $d\theta = 2\pi/V_\theta$, we have $r_{V_r-1} \neq 0$. We therefore calculate up to r_{V_r-2} and simply fix the final vertex at the origin. We can pick the ratio of the number of radial to angular vertices $V_r = \alpha V_\theta = \alpha M$ to approximate the theoretical limiting structure. Then

$$\lim_{M\to\infty} v_M \;=\; \lim_{M\to\infty} v_0 \left(1 - \frac{2\pi}{M}\right)^{\alpha M} \;=\; e^{-2\pi\alpha}. \tag{D6}$$

Setting $\alpha = 2$, then as $M \to \infty$,

$$dr_{\text{last}} \;=\; e^{-4\pi}, \qquad dr_{\text{2nd last}} \;=\; \frac{4\pi}{M}\,dr_{\text{last}} + \mathcal{O}(M^{-2}). \tag{D7}$$

The jump to the origin is nonzero in the limit, while the second last dr does limit to 0. However, this setup is sufficient to show convergence).

Numerical convergence to continuum limit

We now present numerical convergence results for spiderwebs of increasing density from Main Text [3]. We compare numerical solutions of the graph NEP to the continuum solutions:

$$f_{j,0}(r) \;\propto\; \cos\!\big((j + \tfrac{1}{2})\pi\, r\big)\,, \quad k_{j,0} \;=\; \frac{(j + \frac{1}{2})\pi}{\sqrt{1+\gamma}}. \tag{D8}$$

and

$$f_{j,m}(r) \;\propto\; \sqrt{r} J_\nu(\zeta_{j,\nu}\, r), \quad \nu = \sqrt{\gamma\, m^2 + \tfrac{1}{4}}\,, \tag{D9}$$

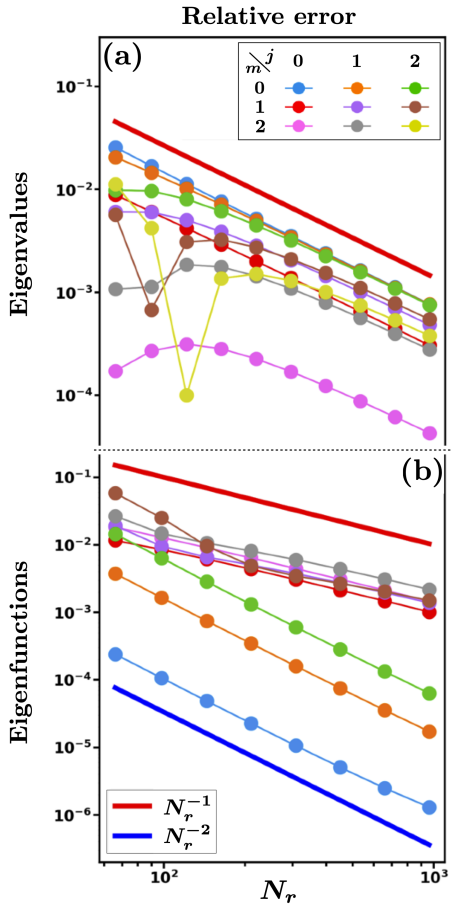


Figure 1. (a) & (b) show graph eigenvalues/eigenmodes converging to the PDE values (eqs. (D9)–(D8)) for increasing numbers N_r of radial vertices. The $m = 0$ modes converge faster than the $m > 0$ solutions.

Appendix E: Discrete homogenization

The Main Text [3] relies on a covering atlas,

$$\mathcal{X} = \{x \subseteq V\}, \quad \text{with} \quad V = \bigcup_{x \in \mathcal{X}} x. \tag{E1}$$

We also define the discrete "partition of unity",

$$\rho_v \;=\; \frac{1}{|\mathcal{X}_v|}, \qquad \mathcal{X}_v \;=\; \{x \in \mathcal{X}\,;\, v \in x\}, \tag{E2}$$

such that

$$\sum_{v \in V} \rho_v \;=\; |V|. \tag{E3}$$

The Main Text relies on the following summation identity,

$$\begin{aligned}\sum_{x,y\in\mathcal{X}}\sum_{v\in x}\sum_{(w\in y)\sim v}\rho_v\,\rho_w &= \sum_{x\in\mathcal{X}}\sum_{v\in x}\rho_v\sum_{y\in\mathcal{X}}\sum_{(w\in y)\sim v}\rho_w\\ &= \sum_{v\in V}\sum_{x\in\mathcal{X}_v}\rho_v\sum_{y\in\mathcal{X}}\sum_{(w\in y)\sim v}\rho_w\\ &= \sum_{v\in V}\sum_{y\in\mathcal{X}}\sum_{(w\in y)\sim v}\rho_w\\ &= \sum_{v\in V}\sum_{w\sim v}\sum_{y\in\mathcal{X}_w}\rho_w\\ &= \sum_{v\in V}\sum_{w\sim v},\end{aligned} \tag{E4}$$

which counts the total number vertices twice. We reorganize the correction problem, eq.(51) in the Main Text [3], into a compact form using Hilbert spaces over the vertex and edge states within $x \in \mathcal{P}(V)$. First, define the ξ state vector,

$$|\xi_x\rangle = \sum_{v\in x}\xi_v\otimes|v\rangle\,, \tag{E5}$$

with the orthonormal basis

$$\langle v|v'\rangle \;=\; \delta_{v,v'}. \tag{E6}$$

We use the tensor product for eq. (E5) because the $\xi_v \in T_xM$ are themselves vectors in the local tangent space. We define the basis for edges in terms of vertex pairs, $v, w \in x$, and a lattice vector $r \in \Lambda_x \subset T_xM$. The basis elements are defined provided $w + r \sim v$ or $v - r \sim w$, with the anti-symmetry

$$|v,w,r\rangle \;=\; -\,|w,v,-r\rangle\,. \tag{E7}$$

We define the edge Hilbert space

$$\mathcal{H}_x = \mathrm{span}\{|v,w,r\rangle\}\,, \tag{E8}$$

where

$$\langle v,w,r|v',w',r'\rangle \;=\; \delta_{v,v'}\,\delta_{w,w'}\,\delta_{r,r'}. \tag{E9}$$

We define the discrete derivative operator,

$$\mathrm{d} \;=\; \frac{1}{2}\sum_{r\in\Lambda_x}\sum_{v,w\in x}|v,w,r\rangle\,(\langle w|-\langle v|)\,, \tag{E10}$$

which takes the $\xi_w - \xi_v$ difference and places the value on every $v \to w + r$ edge. We include the factors of $1/2$ to account for the redundancy resulting in eq. (E7). The correction problem also has inverse length factors; hence we define the proper transposes,

$$|v\rangle^* \;=\; \langle v|\,,\qquad |v,w,r\rangle^* \;=\; \frac{1}{\ell^{(K)}_{v,w+r}}\,\langle v,w,r|\,. \tag{E11}$$

So that $*$ is an involution,

$$\langle v,w,r|^* \;=\; \ell^{(K)}_{v,w+r}\;|v,w,r\rangle\,. \tag{E12}$$

That is, the vertex basis behaves in the simple way one might expect. But the edge-basis transpose is weighted such that, for any state $|t_x\rangle \in \mathcal{H}_x$,

$$|t_x\rangle^* \;=\; \langle t_x|\,\mathrm{K}_x, \tag{E13}$$

where

$$\mathrm{K}_x \;=\; \frac{1}{2}\sum_{r\in\Lambda_x}\sum_{v,w\in x}\frac{1}{\ell^{(K)}_{v,w+r}}\,|v,w,r\rangle\,\langle v,w,r|\,. \tag{E14}$$

We define the right-hand side edge vector

$$|r_x\rangle \;=\; \frac{1}{2}\sum_{r\in\Lambda_x}\sum_{v,w\in x} r\otimes|v,w,r\rangle\,. \tag{E15}$$

Again, we use the tensor product because the lattice is a subset of the tangent space $r\in T_xM$. Both d and $|r_x\rangle$ are invariant under the action $(v,w,r)\to(w,v,-r)$. Finally, the correction problem becomes

$$\mathrm{d}^*\mathrm{d}\,|\xi_x\rangle \;=\; -\mathrm{d}^*\,|r_x\rangle\,, \tag{E16}$$

The difference operator, d, has the constant null-vector,

$$|x\rangle \;=\; \sum_{v\in x}|v\rangle\,. \tag{E17}$$

Eq. (E16) is solvable (non-uniquely) because $\langle x|\,\mathrm{d}^*=0$. We impose the gauge-fixing condition,

$$\langle x|\xi_x\rangle \;=\; 0. \tag{E18}$$

Eq. (E16) is an exact discrete analogue of asymptotic homogenization for PDEs [4–6]. In particular, Eq. (E16) is called the "cell problem" or "corrector equation" for regularizing continuous elliptic operators with rapidly varying non-constant coefficients. Recent work also exists on discrete versions of the homogenization problem [7, 8]. To our knowledge, no work on homogenization yet exists on the continuous limit for metric graphs. Eq. (E16) also takes the simpler form

$$\mathrm{d}^*\,|t_x\rangle = 0, \tag{E19}$$

where

$$|t_x\rangle \;=\; |r_x\rangle + \mathrm{d}\,|\xi_x\rangle\,, \tag{E20}$$

which implies, $|t_x\rangle = (1-\mathrm{d}(\mathrm{d}^*\mathrm{d})^+\mathrm{d}^*)\,|r_x\rangle$ where d^+ is the Moore-Penrose pseudoinverse. However, $\mathrm{d}(\mathrm{d}^*\mathrm{d})^+\mathrm{d}^* = \mathrm{d}\,\mathrm{d}^+$. Therefore,

$$|t_x\rangle \;=\; (1-\mathrm{d}\,\mathrm{d}^+)\,|r_x\rangle \tag{E21}$$

Note the vectors $r_x\in\Lambda_x\subset T_xM$. But in general, $t_x\in T_xM$, but not necessarily the lattice. Eq. (E19) is also equivalent to the Hodge decomposition,

$$|r_x\rangle = -\mathrm{d}\,|\xi_x\rangle + \delta\,|\phi_x\rangle\,, \tag{E22}$$

where δ^* is the "cycle-space" operator [9] such that

$$\delta^*\mathrm{d} = 0. \tag{E23}$$

Therefore,

$$\delta^*\delta\,|\phi_x\rangle = \delta^*\,|r_x\rangle\,, \tag{E24}$$

however, δ has linearly independent columns ($|\phi_x\rangle$ has no gauge freedom), therefore $\delta^*\delta$ is directly invertible and,

$$|t_x\rangle = \delta(\delta^*\delta)^{-1}\delta^*\,|r_x\rangle = \delta\,\delta^+\,|r_x\rangle\,, \tag{E25}$$

where

$$\mathrm{d}\,\mathrm{d}^+ + \delta\,\delta^+ = 1 \tag{E26}$$

Recall $r,\xi_v\in T_xM$ and therefore $|t_x\rangle\in T_xM\otimes\mathcal{H}_x$. Therefore, the regularized edge conductivity tensor,

$$\mathcal{K}(x) \;=\; \mathrm{tr}_{\mathcal{H}_x}(|t_x\rangle\otimes|t_x\rangle)\,, \tag{E27}$$

where $\mathrm{tr}_{\mathcal{H}_x}$ represents the partial trace over $\mathcal{H}_x$ with respect to the metric, K_x. That is, for any $|e\rangle\,,|f\rangle\in\mathcal{H}_x$, and $t,s\in T_xM$,

$$\mathrm{tr}_{\mathcal{H}_x}((t\otimes|e\rangle)\otimes(s\otimes|f\rangle)) \;=\; \langle e|\,\mathrm{K}_x|f\rangle\;t\otimes s. \tag{E28}$$

Unlike in the original case, we lose the direct connection between $\mathrm{tr}(\mathcal{K})$ and $\mathcal{C}$. In all of our examples, we observe $\mathrm{tr}(\mathcal{K})\le\mathcal{C}/d$ (for d the dimension of M); we don't know if this holds in general.

Appendix F: Truncated square graph

The unit graph of the periodic truncated square graph has an adjacency structure,

$$\begin{array}{rcl|l|l|l} v_N & \sim & v_S + e_2 & v_E & v_W \\ v_S & \sim & v_N - e_2 & v_E & v_W \\ v_E & \sim & v_N & v_S & v_W + e_1 \\ v_W & \sim & v_N & v_S & v_E - e_1 \end{array}$$

We order the basis vectors in the vertex and edge Hilbert spaces, respectively, as

$$\{|N\rangle, |S\rangle, |E\rangle, |W\rangle\} \tag{F1}$$

$$\{|N,E,0\rangle, |N,W,0\rangle, |S,E,0\rangle, |S,W,0\rangle, |N,S,a_2\rangle, |E,W,a_1\rangle\}. \tag{F2}$$

The discrete derivative is

$$\begin{aligned} \mathrm{d} = \frac{1}{2}\Big(& |N,E,0\rangle\,(\langle E| - \langle N|) + |N,W,0\rangle\,(\langle W| - \langle N|) + |N,S,a_2\rangle\,(\langle S| - \langle N|) \\ & + |S,E,0\rangle\,(\langle E| - \langle S|) + |S,W,0\rangle\,(\langle W| - \langle S|) + |S,N,-a_2\rangle\,(\langle N| - \langle S|) \\ & + |E,N,0\rangle\,(\langle N| - \langle E|) + |E,S,0\rangle\,(\langle S| - \langle E|) + |E,W,a_1\rangle\,(\langle W| - \langle E|) \\ & + |W,N,0\rangle\,(\langle N| - \langle W|) + |W,S,0\rangle\,(\langle S| - \langle W|) + |W,E,-a_1\rangle\,(\langle E| - \langle W|)\Big). \end{aligned} \tag{F3}$$

Grouping terms by symmetry $|v,w,r\rangle = -\,|w,v,-r\rangle$,

$$\begin{aligned} \mathrm{d} = {} & |N,E,0\rangle\,(\langle E| - \langle N|) + |N,W,0\rangle\,(\langle W| - \langle N|) + |S,E,0\rangle\,(\langle E| - \langle S|) \\ & + |S,W,0\rangle\,(\langle W| - \langle S|) + |N,S,a_2\rangle\,(\langle S| - \langle N|) + |E,W,a_1\rangle\,(\langle W| - \langle E|). \end{aligned} \tag{F4}$$

In matrix form, following the ordering in eqs. (F1)–(F2), we have

$$\mathrm{d} = \begin{bmatrix} -1 & 0 & 1 & 0 \\ -1 & 0 & 0 & 1 \\ 0 & -1 & 1 & 0 \\ 0 & -1 & 0 & 1 \\ -1 & 1 & 0 & 0 \\ 0 & 0 & -1 & 1 \end{bmatrix}, \qquad \text{and} \qquad \mathrm{d}^*\mathrm{d} = \frac{1}{\ell}\begin{bmatrix} 3 & -1 & -1 & -1 \\ -1 & 3 & -1 & -1 \\ -1 & -1 & 3 & -1 \\ -1 & -1 & -1 & 3 \end{bmatrix}. \tag{F5}$$

The discrete Laplacian happens to coincide with a fully connected 4-vertex graph,

$$\mathrm{d}^*\mathrm{d} = \sum_{v,w\in V_x} (4\,\delta_{v,w} - 1)\,|v\rangle\,\langle w|\,. \tag{F6}$$

For the right-hand side,

$$|r_x\rangle = 0 \otimes \big(\,|N,W,0\rangle + |N,S,0\rangle + |S,E,0\rangle + |S,W,0\rangle\,\big) + a_2 \otimes |N,S,a_2\rangle + a_1 \otimes |E,W,a_1\rangle \tag{F7}$$

$$\mathrm{d}^*\,|r_x\rangle = \frac{1}{\ell}\big(a_2 \otimes (|S\rangle - |N\rangle) + a_1 \otimes (|W\rangle - |E\rangle)\,\big), \tag{F8}$$

which in matrix notation is

$$\mathrm{d}^*\,|r_x\rangle = \begin{bmatrix} 0 & -\alpha \\ 0 & \alpha \\ -\alpha & 0 \\ \alpha & 0 \end{bmatrix}, \tag{F9}$$

where $\alpha = \|a_1\| = \|a_2\|$. Altogether, the solution to the corrector equation eq. E16 with the gauge-fixing condition eq. E18 is

$$\mathrm{d}^*\,\mathrm{d}\,|\xi_x\rangle = -\,\mathrm{d}^*\,|r_x\rangle \quad \Rightarrow \quad |\xi_x\rangle = -\frac{\ell}{4}\,\mathrm{d}^*\,|r_x\rangle\,. \tag{F10}$$

We now have

$$|t_x\rangle \;=\; \frac{a_1-a_2}{4}\otimes(|N,E,0\rangle-|S,W,0\rangle)+\frac{a_1+a_2}{4}\otimes(|S,E,0\rangle-|N,W,0\rangle)+\frac{1}{2}\,|r\rangle \;=\; \frac{\alpha}{4}\begin{bmatrix} 1 & -1\\ -1 & -1\\ 1 & 1\\ -1 & 1\\ 0 & 2\\ 2 & 0\end{bmatrix}. \tag{F11}$$

Therefore,

$$\mathcal{K}(x) \;=\; \frac{\alpha^2\ell}{2}I, \qquad \mathcal{C}(x) \;=\; 6\ell. \tag{F12}$$

For completeness,

$$\delta \;=\; \begin{bmatrix} -1 & 1 & 1\\ 0 & -1 & -1\\ 1 & 0 & -1\\ 0 & 0 & 1\\ 0 & 1 & 0\\ 1 & 0 & 0\end{bmatrix}, \qquad \delta^*\delta \;=\; \begin{bmatrix} 3 & -1 & -2\\ -1 & 3 & 2\\ -2 & 2 & 4\end{bmatrix}, \qquad \delta\delta^+ \;=\; \frac{1}{4}\begin{bmatrix} 2 & -1 & -1 & 0 & 1 & -1\\ -1 & 2 & 0 & -1 & -1 & -1\\ -1 & 0 & 2 & -1 & 1 & 1\\ 0 & -1 & -1 & 2 & -1 & 1\\ 1 & -1 & 1 & -1 & 2 & 0\\ -1 & -1 & 1 & 1 & 0 & 2\end{bmatrix}. \tag{F13}$$

Appendix G: Truncated trihexagonal graph

The unit graph of the periodic truncated trihexagonal graph has an adjacency structure,

$$\begin{array}{llllll}
v_0 & \sim & v_1 & , & v_7+e_1 & , & v_{11}\\
v_1 & \sim & v_0 & , & v_2 & , & v_6+e_1\\
v_2 & \sim & v_1 & , & v_3 & , & v_9+e_1-e_2\\
v_3 & \sim & v_2 & , & v_4 & , & v_8+e_1-e_2\\
v_4 & \sim & v_3 & , & v_5 & , & v_{11}-e_2\\
v_5 & \sim & v_4 & , & v_6 & , & v_{10}-e_2
\end{array}
\qquad
\begin{array}{llllll}
v_6 & \sim & v_1-e_1 & , & v_5 & , & v_7\\
v_7 & \sim & v_0-e_1 & , & v_6 & , & v_8\\
v_8 & \sim & v_3-e_1+e_2 & , & v_7 & , & v_9\\
v_9 & \sim & v_2-e_1+e_2 & , & v_8 & , & v_{10}\\
v_{10} & \sim & v_5+e_2 & , & v_9 & , & v_{11}\\
v_{11} & \sim & v_0 & , & v_4+e_2 & , & v_{10}.
\end{array}$$

The graph NEP reduces to $L_x(k)f(V_x)=0$ where $f(V_x)=(\,f_0\;\;f_1\;\;\ldots\;\;f_{11}\,)^\top$ and

$$L_0(k) \;=\; \begin{bmatrix}
-3\gamma & 1 & 0 & 0 & 0 & 0 & 0 & z_1 & 0 & 0 & 0 & 1\\
1 & -3\gamma & 1 & 0 & 0 & 0 & z_1 & 0 & 0 & 0 & 0 & 0\\
0 & 1 & -3\gamma & 1 & 0 & 0 & 0 & 0 & 0 & z_1\bar{z}_2 & 0 & 0\\
0 & 0 & 1 & -3\gamma & 1 & 0 & 0 & 0 & z_1\bar{z}_2 & 0 & 0 & 0\\
0 & 0 & 0 & 1 & -3\gamma & 1 & 0 & 0 & 0 & 0 & 0 & \bar{z}_2\\
0 & 0 & 0 & 0 & 1 & -3\gamma & 1 & 0 & 0 & 0 & \bar{z}_2 & 0\\
0 & \bar{z}_1 & 0 & 0 & 0 & 1 & -3\gamma & 1 & 0 & 0 & 0 & 0\\
\bar{z}_1 & 0 & 0 & 0 & 0 & 0 & 1 & -3\gamma & 1 & 0 & 0 & 0\\
0 & 0 & 0 & \bar{z}_1z_2 & 0 & 0 & 0 & 1 & -3\gamma & 1 & 0 & 0\\
0 & 0 & \bar{z}_1z_2 & 0 & 0 & 0 & 0 & 0 & 1 & -3\gamma & 1 & 0\\
0 & 0 & 0 & 0 & 0 & z_2 & 0 & 0 & 0 & 1 & -3\gamma & 1\\
1 & 0 & 0 & 0 & z_2 & 0 & 0 & 0 & 0 & 0 & 1 & -3\gamma
\end{bmatrix}, \tag{G1}$$

where $z_j=e^{i\vartheta_j}$. Setting the determinant,

$$\det\left(L_0(k)\right)=\sum_{j=0}^{6}(-9\gamma^2)^j\,\mathrm{D}_{2j} \;=\; 0 \qquad \text{where} \qquad \begin{array}{rcl}
\mathrm{D}_0 &=& (3\gamma_{\mathrm{H}})^4,\\
\mathrm{D}_2 &=& 4(3\gamma_{\widetilde{\mathrm{H}}})^2+30(3\gamma_{\mathrm{H}})^2,\\
\mathrm{D}_4 &=& 3\left(10(3\gamma_{\mathrm{H}})^2+59\right),\\
\mathrm{D}_6 &=& 6(3\gamma_{\mathrm{H}})^2+262,\\
\mathrm{D}_8 &=& 111,\\
\mathrm{D}_{10} &=& 18,\\
\mathrm{D}_{12} &=& 1,
\end{array} \tag{G2}$$

where, $\gamma_{\rm H}$ is the hexagon solution from eq. (34) of the Main Text [3] and,

$$\gamma_{\rm H} \,=\, \frac{|1+e^{i\vartheta_1}+e^{i\vartheta_2}|}{3}, \qquad \gamma_{\widetilde{\rm H}} \,=\, \frac{|1+e^{i(\vartheta_1-2\vartheta_2)}+e^{i(2\vartheta_1-\vartheta_2)}|}{3}. \tag{G3}$$

The lattice vectors are

$$a_1,\, a_2 \,=\, \frac{(3+\sqrt{3})\ell}{2}\,(\sqrt{3},\pm 1). \tag{G4}$$

As $\ell \to 0$, the limiting dispersion relation,

$$k^2 \,=\, \frac{2+\sqrt{3}}{4}\,\frac{\kappa\cdot\kappa}{2} + \mathcal{O}(\ell^2), \tag{G5}$$

where $(2+\sqrt{3})/4 \approx 0.933013$. The effective dimension is $d_{\rm eff.} \approx 2.14359$. For the homogenized PDE, we have

$$\begin{aligned}
{\rm d} \,=\, & \\
& |0,1,0\rangle\,(\langle 0| - \langle 1|)+ \\
& |1,2,0\rangle\,(\langle 1| - \langle 2|)+ \\
& |2,3,0\rangle\,(\langle 2| - \langle 3|)+ \\
& |3,4,0\rangle\,(\langle 3| - \langle 4|)+ \\
& |4,5,0\rangle\,(\langle 4| - \langle 5|)+ \\
& |5,6,0\rangle\,(\langle 5| - \langle 6|)+ \\
& |6,7,0\rangle\,(\langle 6| - \langle 7|)+ \\
& |7,8,0\rangle\,(\langle 7| - \langle 8|)+ \\
& |8,9,0\rangle\,(\langle 8| - \langle 9|)+ \\
& |9,10,0\rangle\,(\langle 9| - \langle 10|)+ \\
& |10,11,0\rangle\,(\langle 10| - \langle 11|)+ \\
& |11,0,0\rangle\,(\langle 11| - \langle 0|)+ \\
& |0,7,a_1\rangle\,(\langle 0| - \langle 7|)+ \\
& |1,6,a_1\rangle\,(\langle 1| - \langle 6|)+ \\
& |10,5,a_2\rangle\,(\langle 10| - \langle 5|)+ \\
& |11,4,a_2\rangle\,(\langle 11| - \langle 4|)+ \\
& |8,3,a_2-a_1\rangle\,(\langle 8| - \langle 3|)+ \\
& |9,2,a_2-a_1\rangle\,(\langle 9| - \langle 2|)
\end{aligned} \tag{G6}$$

$$\mathrm{d} = \begin{bmatrix}
1 & -1 & 0 & 0 & 0 & 0 & 0 & 0 & 0 & 0 & 0 & 0 \\
0 & 1 & -1 & 0 & 0 & 0 & 0 & 0 & 0 & 0 & 0 & 0 \\
0 & 0 & 1 & -1 & 0 & 0 & 0 & 0 & 0 & 0 & 0 & 0 \\
0 & 0 & 0 & 1 & -1 & 0 & 0 & 0 & 0 & 0 & 0 & 0 \\
0 & 0 & 0 & 0 & 1 & -1 & 0 & 0 & 0 & 0 & 0 & 0 \\
0 & 0 & 0 & 0 & 0 & 1 & -1 & 0 & 0 & 0 & 0 & 0 \\
0 & 0 & 0 & 0 & 0 & 0 & 1 & -1 & 0 & 0 & 0 & 0 \\
0 & 0 & 0 & 0 & 0 & 0 & 0 & 1 & -1 & 0 & 0 & 0 \\
0 & 0 & 0 & 0 & 0 & 0 & 0 & 0 & 1 & -1 & 0 & 0 \\
0 & 0 & 0 & 0 & 0 & 0 & 0 & 0 & 0 & 1 & -1 & 0 \\
0 & 0 & 0 & 0 & 0 & 0 & 0 & 0 & 0 & 0 & 1 & -1 \\
-1 & 0 & 0 & 0 & 0 & 0 & 0 & 0 & 0 & 0 & 0 & 1 \\
0 & 1 & 0 & 0 & 0 & 0 & -1 & 0 & 0 & 0 & 0 & 0 \\
1 & 0 & 0 & 0 & 0 & 0 & 0 & -1 & 0 & 0 & 0 & 0 \\
0 & 0 & 0 & 0 & -1 & 0 & 0 & 0 & 0 & 0 & 0 & 1 \\
0 & 0 & 0 & 0 & 0 & -1 & 0 & 0 & 0 & 0 & 1 & 0 \\
0 & 0 & -1 & 0 & 0 & 0 & 0 & 0 & 0 & 1 & 0 & 0 \\
0 & 0 & 0 & -1 & 0 & 0 & 0 & 0 & 1 & 0 & 0 & 0
\end{bmatrix} \tag{G7}$$

$$\mathrm{d}^*\mathrm{d} = \frac{1}{\ell}\begin{bmatrix} 3 & -1 & 0 & 0 & 0 & 0 & 0 & -1 & 0 & 0 & 0 & -1 \\ -1 & 3 & -1 & 0 & 0 & 0 & -1 & 0 & 0 & 0 & 0 & 0 \\ 0 & -1 & 3 & -1 & 0 & 0 & 0 & 0 & 0 & -1 & 0 & 0 \\ 0 & 0 & -1 & 3 & -1 & 0 & 0 & 0 & -1 & 0 & 0 & 0 \\ 0 & 0 & 0 & -1 & 3 & -1 & 0 & 0 & 0 & 0 & 0 & -1 \\ 0 & 0 & 0 & 0 & -1 & 3 & -1 & 0 & 0 & 0 & -1 & 0 \\ 0 & -1 & 0 & 0 & 0 & -1 & 3 & -1 & 0 & 0 & 0 & 0 \\ -1 & 0 & 0 & 0 & 0 & 0 & -1 & 3 & -1 & 0 & 0 & 0 \\ 0 & 0 & 0 & -1 & 0 & 0 & 0 & -1 & 3 & -1 & 0 & 0 \\ 0 & 0 & -1 & 0 & 0 & 0 & 0 & 0 & -1 & 3 & -1 & 0 \\ 0 & 0 & 0 & 0 & 0 & -1 & 0 & 0 & 0 & -1 & 3 & -1 \\ -1 & 0 & 0 & 0 & -1 & 0 & 0 & 0 & 0 & 0 & -1 & 3 \end{bmatrix} \tag{G8}$$

Also,

$$\delta = \begin{bmatrix} 0 & 0 & 0 & 0 & -1 & 0 & 1 \\ 0 & 0 & 0 & 0 & -1 & -1 & 1 \\ 0 & 1 & 0 & 0 & -1 & -1 & 1 \\ 1 & 1 & 0 & 0 & -1 & -1 & 1 \\ 1 & 1 & 0 & 1 & -1 & -1 & 1 \\ 1 & 1 & 1 & 1 & -1 & -1 & 1 \\ 1 & 1 & 1 & 1 & -1 & 0 & 1 \\ 1 & 1 & 1 & 1 & 0 & 0 & 1 \\ 0 & 1 & 1 & 1 & 0 & 0 & 1 \\ 0 & 0 & 1 & 1 & 0 & 0 & 1 \\ 0 & 0 & 0 & 1 & 0 & 0 & 1 \\ 0 & 0 & 0 & 0 & 0 & 0 & 1 \\ 0 & 0 & 0 & 0 & 0 & 1 & 0 \\ 0 & 0 & 0 & 0 & 1 & 0 & 0 \\ 0 & 0 & 0 & 1 & 0 & 0 & 0 \\ 0 & 0 & 1 & 0 & 0 & 0 & 0 \\ 0 & 1 & 0 & 0 & 0 & 0 & 0 \\ 1 & 0 & 0 & 0 & 0 & 0 & 0 \end{bmatrix}, \qquad \text{with} \qquad \delta^*\delta = \begin{bmatrix} 6 & 5 & 3 & 4 & -4 & -3 & 5 \\ 5 & 8 & 4 & 5 & -5 & -4 & 7 \\ 3 & 4 & 6 & 5 & -2 & -1 & 5 \\ 4 & 5 & 5 & 8 & -3 & -2 & 7 \\ -4 & -5 & -2 & -3 & 8 & 5 & -7 \\ -3 & -4 & -1 & -2 & 5 & 6 & -5 \\ 5 & 7 & 5 & 7 & -7 & -5 & 12 \end{bmatrix} \tag{G9}$$

Appendix H: Uncertainty on the log scale

A general log-log plot shows $\log(y)$ versus $\log(x)$ for positive $y > 0$; in our case relative errors. However, showing *uncertainty* on a log-log plot by including $y \pm \Delta y$ (where e.g. Δy is the standard deviation) fails when $y - \Delta y \leq 0$. We instead display uncertainty by plotting $\log(y) \pm \Delta\log(y)$ [10]. To leading order,

$$\Delta\log(y) \approx \log\left(1 + \frac{\Delta y}{y}\right). \tag{H1}$$

Therefore,

$$\log(y) \pm \Delta\log(y) \approx \begin{cases} \log(y + \Delta y) & \Delta y > 0 \\ \log(y/(1 + \Delta y/y)) & \Delta y < 0. \end{cases} \tag{H2}$$

Appendix I: The numerical convergence to isotropy

The deviatoric conductivity is defined as

$$\Sigma = \frac{\mathcal{K}}{\mathrm{tr}(\mathcal{K})} - \frac{1}{d}I. \tag{I1}$$

For a graphs G_n of increasing densities, we show that the deviatoric conductivity $\|\Sigma_n\| \to 0$; see figure 2. Therefore, $\mathcal{K}_n \propto I$, where I is the identity.

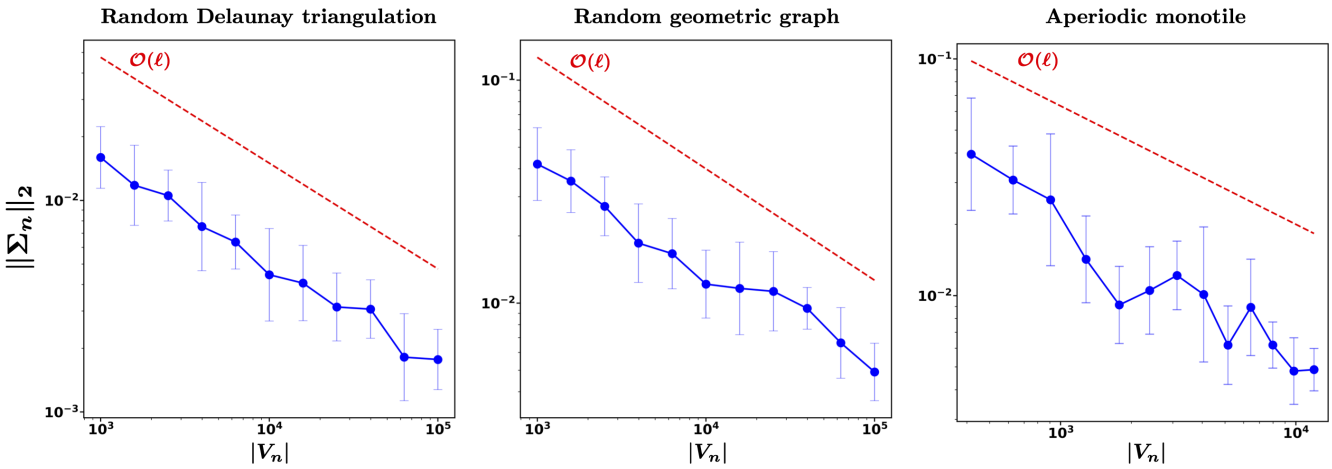


Figure 2. The deviatoric conductivity, $\Sigma_n = \mathcal{O}(\ell)$ as $|V_n| \to \infty$ and $\ell \to 0$. We display uncertainties in log-space as defined in §H.

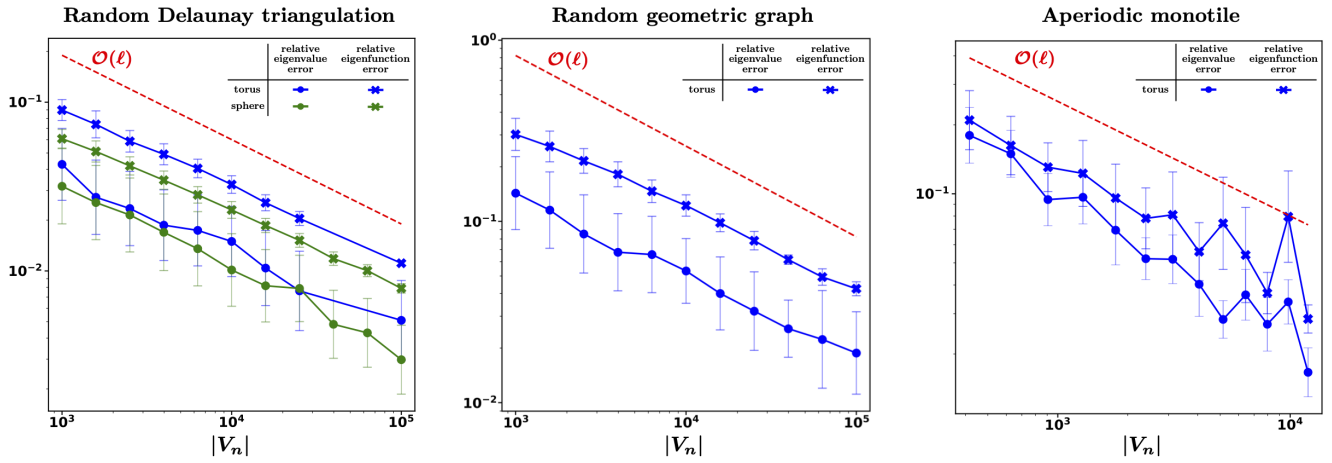


Figure 3. Fundamental graph eigenmodes converge to continuum limits for various space-filling random graphs. We show the relative absolute error between graph and PDE eigenvalues and eigenvectors. We display uncertainties in log-space as defined in §H.

Appendix J: Numerical convergence for random graphs

We demonstrate numerical convergence of the graph eigenmodes to the PDE eigenmodes for the graphs of section §Random Graphs (see [3]). For the graph NEP, we conduct a high-density search in the range $0 < k < 10$ (expecting values near $0 < \pi\sqrt{2\mathcal{D}} < 10$). For each NEP eigenpair $(k, f(V))$, we construct the corresponding graph eigenfunction, f^G. Because the $f_{m,n}$ eigenfunctions are all mutually degenerate (*i.e.*, $\lambda_{m,n} = 4\pi^2\mathcal{D}$), any linear combination is an equally valid continuum mode. Therefore, for each mode on G, we construct its manifold equivalent,

$$f^M = \sum_{m,n} \frac{\langle f^G, f_{m,n}\rangle_G}{\|f_{m,n}\|_G^2} f_{m,n}, \tag{J1}$$

where $\langle f, g\rangle_G = \sum_{e\in E} \int_e f\,\overline{g}\,\mathrm{d}x_e$ and the $f_{m,n}$ functions are restricted to the graph. We rank each eigenpair $(k, f(V))$ by the relative eigenvalue and eigenfunction errors, $\mathcal{E}_\lambda = \frac{|k^2-\lambda|}{|\lambda|}$ and $\mathcal{E}_f = \frac{\|f^G - f^M\|_G}{\|f^M\|_G}$, where the denominators in each case are for the manifold values, *i.e.*, the theoretical limiting values. The four smallest errors determine the eigenmodes to compare against the continuum solutions. Figure 3 shows the convergence (blue) of the graph eigenmodes to the PDE eigenmodes, with approximate $\mathcal{O}(\ell)$ scaling. For each graph size, $|V_n|$, we plot the ensemble mean of $\mathcal{E}_\lambda$ and $\mathcal{E}_f$ along with the $\log_{10}$-scaled standard deviations (§H). Figure 3 shows the split eigenvalues converge to a single limit.

Lastly, when searching for NEP eigenvalues, we see clusters of the same size as the continuum multiplicity near each continuum eigenvalue. The same situation applies for higher-wavenumber modes for increasing vertex density.

Appendix K: Continuum limit for an inhomogeneous random graph

We construct an inhomogeneous random graph by randomly sampling the annulus $0.1 \leq r \leq 1$ from the density $\rho(r,\theta) = (0.02 + r^2)(1.02 + \cos(5\theta))$. The graph has $200,000$ vertices and is illustrated in figure 4(a). We place coarse-grained coordinates x lying on an $N_r \times N_\theta = 16 \times 64$ polar grid (in red in figure 4(b)). We scale patches (in orange in figure 4) centered at each x so that each contains $|x| = 300 \pm 4$ vertices. We measure $\mathcal{K}, \mathcal{C}$ and μ at x as illustrated in figure 5. We assume $\mu\mathcal{K}$ and $\mu\mathcal{C}$ are separable as

$$\mu\mathcal{K} \approx \begin{bmatrix} p_0(r) & 0 \\ 0 & p_1(r) \end{bmatrix} q(\theta) \tag{K1}$$

$$\mu\mathcal{C} \approx p_2(r) q(\theta). \tag{K2}$$

The continuum PDE itself is then separable. Setting $f(r,\theta) = R(r)T(\theta)$, the resulting ODEs are

$$\partial_\theta(q(\theta)\partial_\theta T(\theta)) = \nu q(\theta) T(\theta), \qquad T(\theta) = T(\theta + 2\pi), \tag{K3}$$

$$r\partial_r(r p_0(r)\partial_r R(r)) = (\nu p_1(r) - \lambda r^2 p_2(r)) R(r), \qquad R(0.1) = R(1) = 0. \tag{K4}$$

To construct the p_i and q, we interpolate averages of $\mu\mathcal{C}$ and $\mu\mathcal{K}$ in each dimension (after rescaling both my $\max(\mu\mathcal{C})$). We obtain

$$p_0(r) = 0.00178297 + 0.0521971 r \tag{K5}$$

$$p_1(r) = 0.000942758 + 0.0526548 r \tag{K6}$$

$$p_2(r) = 0.00939337 + 0.116148 r \tag{K7}$$

$$q(\theta) = 1 + 0.574\cos(5\,\theta) - 0.0720\cos(10\,\theta) + 0.0177\cos(15\,\theta)\,. \tag{K8}$$

We show the data and respective fits in figure 6. We obtain residuals in eqs. K1-K2 of approximately 5% and 8% respectively–justifying the separation of variables. We show the first several eigenmode comparisons in figure 7. We see relative errors in both the eigenvalues and eigenfunctions of less than 6%. As in the homogeneous random graphs (§J), we see splittings in the degenerate continuum modes, comparing eigenmodes as in eq.J1.

[1] M. S., Linear and Multilinear Algebra **71**, 16 (2022).
[2] X.-P. C. and H. D., East Asian Journal on Applied Mathematics **8**, 139 (2018).
[3] `Main_Text` (2025).
[4] G. Allaire, SIAM Journal on Mathematical Analysis **23**, 1482–1518 (1992).
[5] G. Nguetseng, Zeitschrift für Analysis und ihre Anwendungen **22**, 73–108 (2003).
[6] G. Nguetseng, Zeitschrift für Analysis und ihre Anwendungen **23**, 483–508 (2004).
[7] M. Biskup, Probability Surveys **8** (2011).
[8] A. Gloria, ESAIM: Mathematical Modelling and Numerical Analysis **46**, 1–38 (2011).
[9] J. L. Gross, J. Yellen, and M. Anderson, *Graph Theory and Its Applications* (Chapman and Hall/CRC, 2018).
[10] J. R. Taylor, *Introduction to Error Analysis, second edition*, 2nd ed. (University Science Books, Sausalito, CA, 1997).

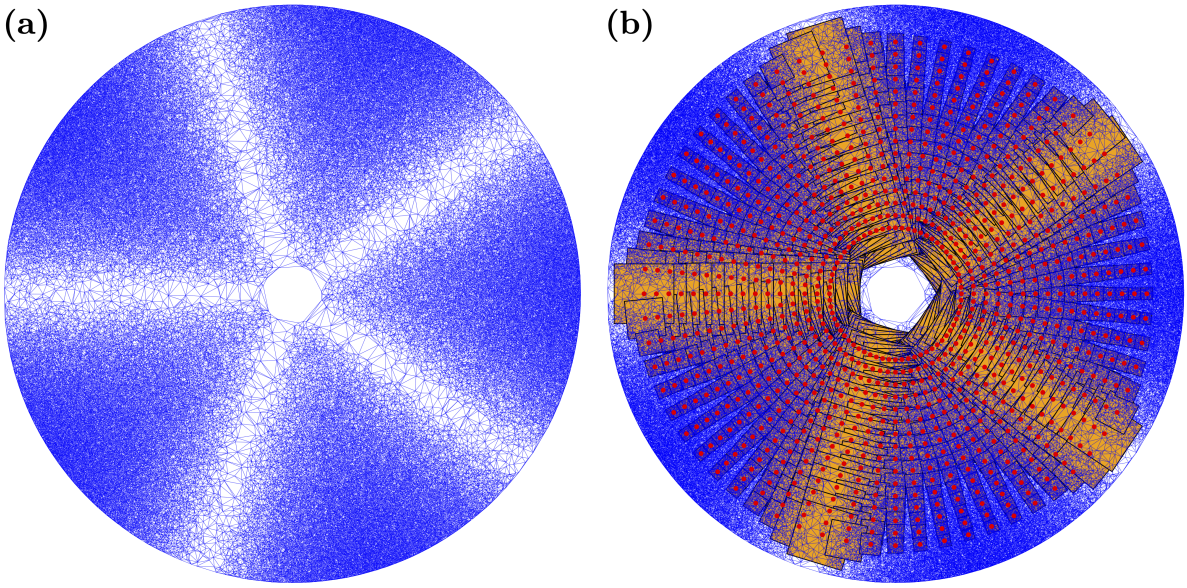


Figure 4. Inhomogeneous random graph and a partial covering. (a) Inhomogeneous random graph with 200k vertices with a radial density $\propto r^2$ and an angular density $1.02+\cos(5\theta)$ (§K). (b) Coarse-grained x vertices (in red) lie on an $N_r \times N_\theta = 16\times 64$ polar grid. We select patches (in orange) centered at each x which each cover approximately 300 vertices v.

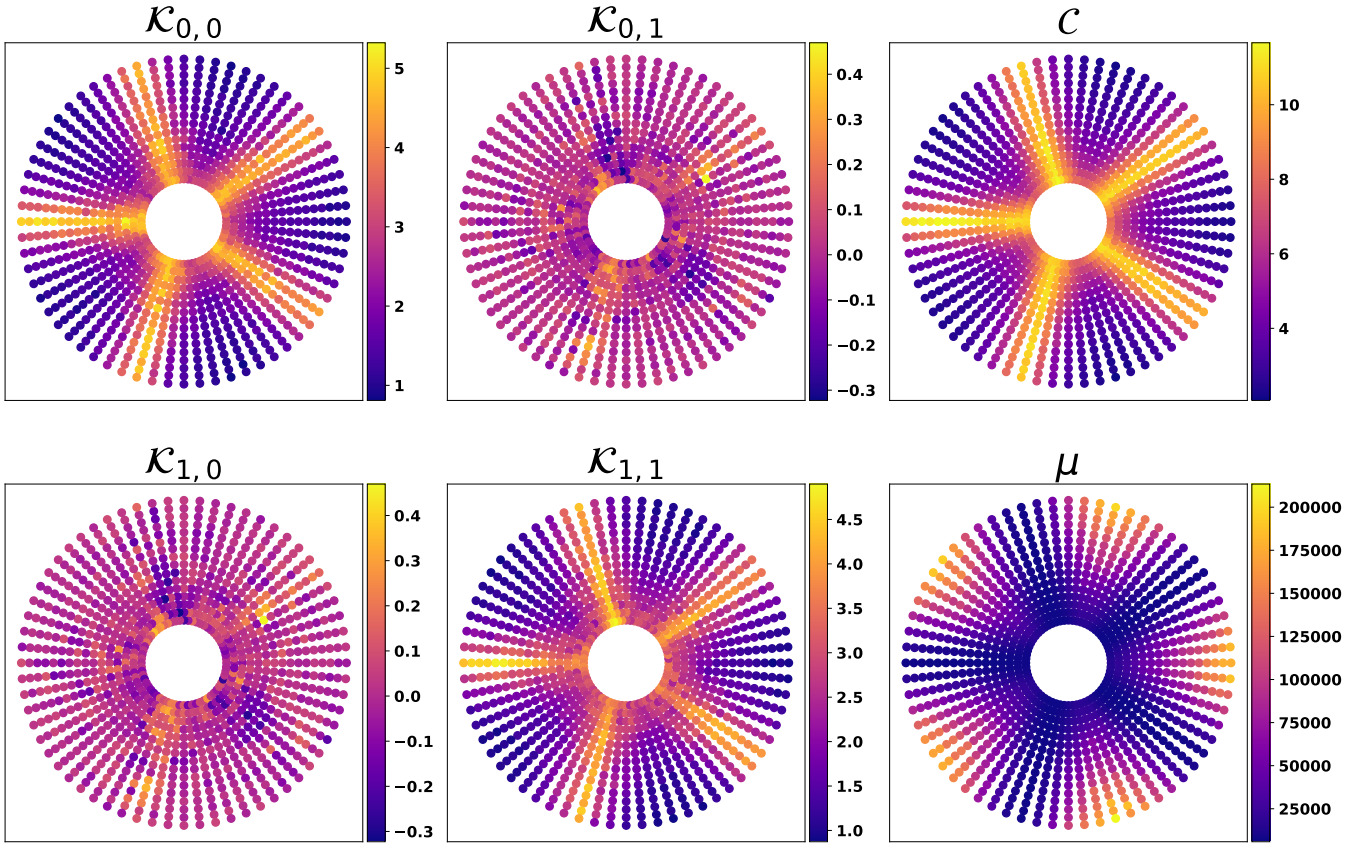


Figure 5. Measurements of the $\mathcal{K}$ components, $\mathcal{C}$, and μ on the coarse-grained coordinates x (in red in figure 4).

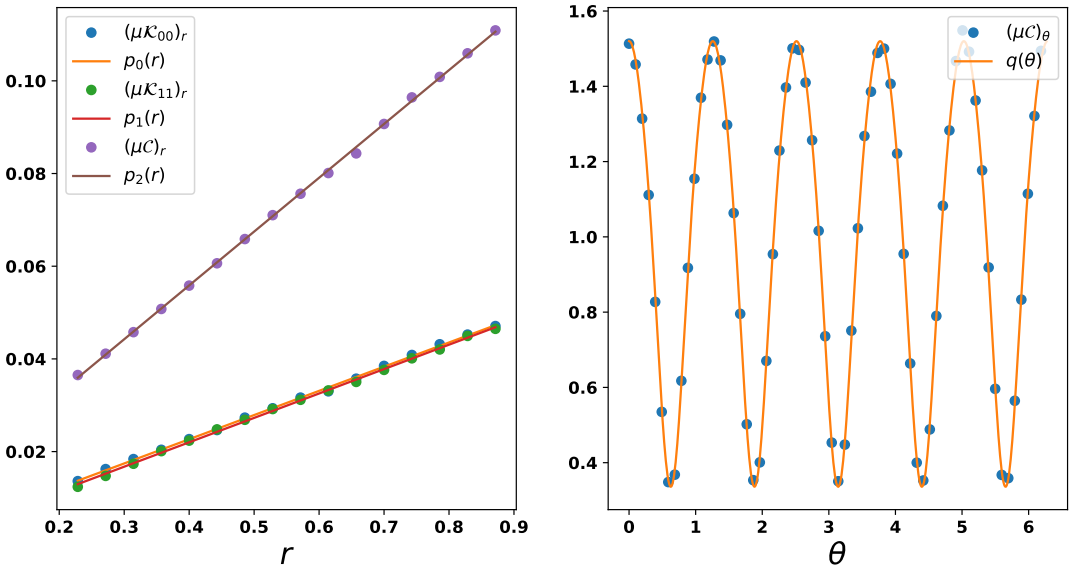


Figure 6. We fit the means of $\mu\mathcal{K}$ and $\mu\mathcal{C}$ in each dimension. We find linear fits $p_i(r)$ for the means over θ of the diagonal component of $\mu\mathcal{K}$ and $\mu\mathcal{C}$, and a cosine fit $q(\theta)$ for the radial mean of $\mu\mathcal{C}$. The fits are expressed in eqs. K5-K8.

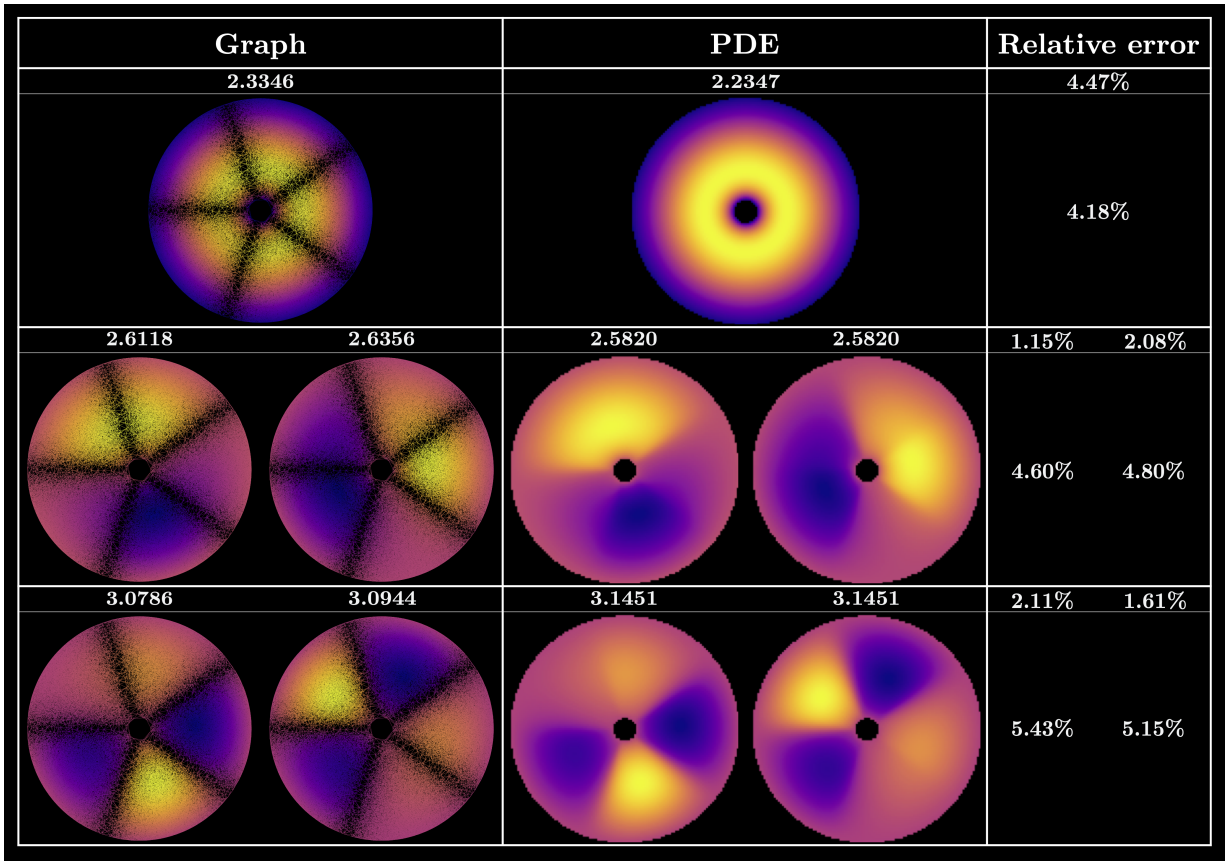


Figure 7. Eigenmode comparisons between the graph and PDE models for the inhomogenenous random graph. Each row for comparison is split into subrows: the top subrow contains the eigenvalues and the bottow subrow containes the eigenfunctions.